Energy 93 (2015) 2384–2394

Contents lists available at ScienceDirect

Energy

journal homepage: www.elsevier.com/locate/energy

Experimental investigation of pyrolysis of rice straw using bench-scale auger, batch and fluidized bed reactors

Hyungseok Nam [a, *], Sergio C. Capareda [a], Nanjappa Ashwath [a, b], Jinjuta Kongkasawan [a]

[a] Biological and Agricultural Engineering Department, Texas A&M University, College Station, TX 77843, USA
[b] School of Medical and Applied Sciences, Central Queensland University, Rockhampton, QLD 4702, Australia

ARTICLE INFO

Article history:
Received 21 May 2015
Received in revised form
8 October 2015
Accepted 11 October 2015
Available online 19 November 2015

ABSTRACT

Energy conversion efficiencies of three pyrolysis reactors (bench-scale auger, batch, and fluidized bed) were investigated using rice straw as the feedstock at a temperature of 500 °C. The highest bio-oil yield of 43% was obtained from the fluidized bed reactor, while the maximum bio-char yield of 48% was obtained from the batch reactor. Similar bio-oil yields were obtained from the auger and batch type reactors. The GCMS and FTIR were used to evaluate the liquid products from all reactors. The best quality bio-oil and bio-char from the batch reactor was determined to have a heating value of 31 MJ/kg and 19 MJ/kg, respectively. The highest alkali mineral was found in the bio-char produced from the auger reactor. The energy conversion efficiencies of the three reactors indicated that the majority of the energy (50–64%) was in the bio-char products from the auger and batch reactors, while the bio-oil from the fluidized bed reactor contained the highest energy (47%). A Sankey diagram has been produced to show the flows of product energy from each pyrolysis process. The result will help determine which conversion process would be optimal for producing specific products of bio-char, bio-oil, and gas depending on the needs.

1. Introduction

Rice is a major agricultural crop in Asia. Globally, 727 million tons of rice straw were produced in 2009 [1]. Rice production in the United States was ranked 13th in 2012 [2]. Rice straw can be used as feed or bedding material for cattle, and it can also be used in composting. However, rice straw in many underdeveloped or developing countries is left on the ground or burned, and thus will have negative environmental impact [3]. Furthermore, the high SiO_2 and alkali metal content of the straw often causes erosion in the milling apparatus and they also cause slagging or fouling problems in the heat exchangers.

Pyrolysis is a thermochemical process with a temperature range from 300 to 600 °C in an oxygen free condition. The rate at which the thermal decomposition occurs will determine the resulting products depending on the feedstock, temperature, residence time, reactor type and heat transfer. It is widely known that bio-oil and bio-char are the key products from the pyrolysis process. Many studies have used the chemical composition of a lignocellulosic biomass to understand the relationship between mass and energy yields to external conditions such as temperature, residence time, moisture, and input gas type [4–7]. Among the chemical compositions of the feedstock (cellulose, hemicellulose and lignin), lignin is the most difficult component to convert chemically [8]. Most cellulose, hemicellulose and some lignin degrade into various chemicals in the pyrolysis process, mostly resulting as phenolic compounds with alcohols, acids, aldehydes, ketones, esters, furans and other aromatics [9,10].

The pyrolysis process using the abundant rice waste (rice husk and rice straw) has been done by many researchers. Pyrolysis of rice husk in a fixed bed reactor for a comparison of slow and fast pyrolysis was completed and the maximum bio-oil yield was achieved at 50.5 wt% at 500 °C [11]. The yield of bio-oil from rice straw pyrolysis increased from 30% to 40%, whereas the bio-char yield decreased from 58% to 40% in the lab-scale slow pyrolyzer, as the temperature rose from 300 to 700 °C [12]. Torrefaction, another term for pyrolysis under the temperature from 200 to 300 °C, was experimentally investigated using rice straw through a batch reactor [13].

Several types of reactors were used in the pyrolysis process; an auger type [14–17], a batch type [11,12,18,19], a fluidized bed type [20–22], and a microwave type reactor [23–26]. A fixed bed batch reactor was used to investigate the effects of independent variables

* Corresponding author. Tel.: +19796767111.
E-mail addresses: namhs219@gmail.com (H. Nam), scapareda@tamu.edu (S.C. Capareda).

http://dx.doi.org/10.1016/j.energy.2015.10.028
0360-5442/

of temperature, particle size, nitrogen flow rate, and steam velocity on the pyrolysis products. According to Pütün et al. [18], the maximum yield of bio-oil (35.86%) was through steam pyrolysis. The conditions for maximum bio-oil yields were a temperature of 824 K, a particle size of $0.435 < D < 0.85$ mm, and a nitrogen gas flow of 400 ml/min. Ingram et al. [17] determined that the bio-oil heating value from pine and oak wood from the auger reactor was at a range of 18–22 MJ/kg. The product mass yields of pine woodchips from the auger pyrolysis reactor were 57% liquid and 26% solid [14]. Sadaka et al. [15] used the auger reactor for gasification of agricultural residues. The effect of temperature was tested to produce gas to explore the possibility of finding a fuel source for an on-site facility. Fast pyrolysis in a fluidized bed reactor was used to process rice straw and rice husk at temperatures of 375–500 °C [22]. The highest mass yield of bio-oil from rice straw and rice husk was obtained at 500 °C while the highest char yield was achieved at 375 °C. The fluidized bed reactor was also used for gasification process to convert wastes of sorghum, cotton, gin trash, and dairy manure [20,21]. The microwave reactor was also used to pyrolyze rice straw at 237–423 °C [23]. Furthermore, Lam et al. [24–26] used a microwave pyrolyzer to convert waste engine oil into potential fuel products by reducing metals. The addition of the metallic-char catalyst enhanced the quality of liquid and gas products. Duman et al. [27] used cherry seed to compare slow and fast pyrolysis. The maximum bio-oil yield at 500 °C was found to be about 44 wt% for the fast process and about 15 wt% for the slow pyrolysis.

Many alternative uses of rice straw wastes have been reported recently [28]. Rice straw has excellent potential for soil erosion control, sediment traps, and soil improvement. The straw prevents water erosion and soil loss by retaining moisture, reducing evaporation, controlling soil temperature, preserving fertilizer, and providing useful soil organic matter as it decomposes. Grantz et al. [29] demonstrated that the use of recalcitrant mulch, including straw, improved the growth of plants in arid and semiarid lands. Also, covering soil with a thick layer of straw helps in weed control. Other alternative applications of rice straw include paper and composite materials. According to FAO, 15.6 million tons of non-wood fibers were used for paper and pulp production in the world. Interestingly, the production of rice straw exceeds its use every year. A large amount of rice straw in many underdeveloped or developing countries has often been left as is or burned in the field. The applications mentioned above still produce other types of wastes. Pyrolysis technologies not only help control mass production of rice straw wastes, but they also assist in converting the wastes into valuable soil amendments and catalysts with a deoxidized bio-char. Also, the bio-oil and the gas generated during pyrolysis can be used in power generation. Thus, the comparison of energy conversion efficiencies of different pyrolysis technologies would be of great significance in making use of the rice straw for soil amendment and production of value added products.

The specific objectives of this study were to compare the pyrolysis process using an auger type, a batch type, and a fluidized bed type reactor. The characteristics of rice straw was assessed and used in understanding pyrolysis process and to evaluate solid, liquid and gas product properties. Mass and energy recovery efficiencies were investigated and compared between the reactors. A study of pyrolysis behavior using different reactors will help select right technology for generating a desired pyrolysis product.

2. Materials and experimental methods

2.1. Sample preparation and characterization

Rice straw was obtained from Beaumont, Texas, and air-dried. A Wiley Laboratory mill (model #4) was used to mill the sample using 2-mm sieve. The methods described in Section 2.3 were used for the proximate analysis, high heating value (HVV) and elemental analysis.

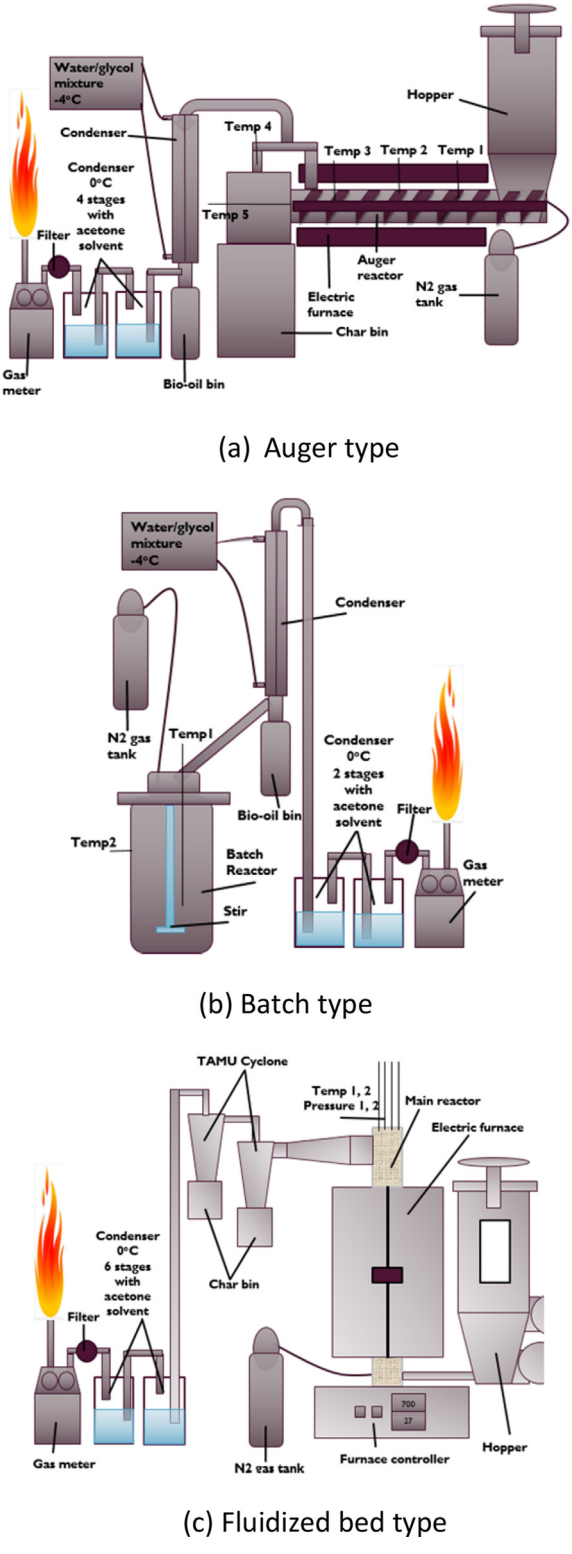

Fig. 1. Schematic diagrams of the three pyrolysis reactors.

2.2. Experimental conditions and equipment

Pyrolysis experiments were conducted using an auger type, a batch type, and a fluidized bed (FB) type reactor as shown in Fig. 1. The auger and batch type reactors will represent slow pyrolysis, and the fluidized bed type reactor represents fast pyrolysis, according to EIA bioenergy group report [30]. The auger type reactor can also be defined as intermediate pyrolysis as the residence time ranged between 20 and 25 min, which is an intermediate residence time between slow pyrolysis (over 4 h) and fast pyrolysis (less than 1 s). All three reactors are regarded as bench-scale reactors, as the maximum processing rate of 100 g/min in auger reactor, 80 g/min in FB reactor, and the one time processing capacity of 300 g in batch reactor can be used.

An auger based reactor was used for slow or intermediate pyrolysis. A 3-zone cylindrical electric furnace (Linberg/Blue M from Thermoelectron Corporation/Centigrate Service Inc., North Carolina) was used to heat the main tube reactor of 10.2 cm diameter and 150 cm length with an auger flight connected to the feed hopper (61 cm × 61 cm × 130 cm). Nitrogen gas of 10 L/min was passed into the reactor during the experiment to make sure that the produced gas was pushed into the exhaust pipe. One K-type thermocouple was placed inside the tube reactor to measure the actual reaction temperature, along with three thermocouples which were attached to the electric furnace. A bio-char bin was fitted at the end of the tube reactor. Two outlets were provided to collect volatile gas from the tube reactor. Glycol water at −4 °C was used to condense the bio-oil in an indirect heat exchange condenser. Then, a four-staged solvent condenser was placed to capture the remaining condensable volatile matter. The feed rate was set at about 10 g/min. The number of solvent condensers used were determined based on a preliminary experiment. The volumetric gas flow was measured with a gas meter (METRIS 250, Itron, Oweenton, KY) after calibration. Then, the sampled gas was analyzed using a gas chromatograph (GC) equipped with thermal conductivity detector (TCD).

A stainless steel batch type reactor (Series 4580 HP/HT, Parr Instrument Company, Moline, IL; Fig. 1) was used for slow pyrolysis. The same set up was used in previous torrefaction study of rice straw and cotton stalk from California [13]. A cylindrical electric furnace was used to heat the 5.7 L AISI 316 reactor and the temperature of the reactor was controlled by a J type thermocouple placed inside the reactor. A chiller using −4 °C glycol water was connected to an indirect heat exchange condenser, and the condensable volatiles were collected in the condenser. The remaining condensable vapors were captured by a two-staged solvent condensers. The remaining incondensable vapor from the condenser was passed through a gas meter and quantified. Nitrogen gas was used to flush out the air in the reactor after the reactor was closed. An internal stirrer was used to mix the sample in the reactor. The temperature was increased to the set temperature (500 °C) at the rate of 4 °C/min. The sampled gas was injected in to a GC-TCD to determine its gas compositions.

A fluidized bed reactor was used for fast pyrolysis. The 30 cm single zone split tube furnace was placed to heat the main tube reactor made of AISI 316 stainless steel. The tube reactor was of the size 7.6 cm diameter and 84 cm long. A K-type thermocouple and a pressure gauging tube were located at the bottom bed, and another thermocouple and gauge were placed at the upper bed. An inert gas, nitrogen, was used for the fluidization of the bed material of Mulgrain 47−10 × 18 (C E Minerals, Andersonville, GA), which used for the previous gasification studies [20,21]. The bed material was sieved using −20 and + 40 mesh sieve pans (ASTM E-11 specification, Fisher Scientific Company, USA). The average density and mean diameter were 1.45 g/mL and 630 μm, respectively. The height of the bed material was 33 cm. The ground rice straw sample was inserted into the main reactor through a 4 cm diameter screw auger feeding system connected to the hopper. The feed rate was set at 5 g/min. Two-stage TAMU cyclones, designed for the pyrolysis process, were connected to the end of the reactor to remove the solid product. The bio-oil was condensed in a six-staged condenser; the first canister was empty, whereas the others contained solvents (acetone). The incondensable gas was passed through the gas meter, and the gas samples were collected and analyzed using a GC-TCD.

2.3. Analytical methods

The solid, liquid, and gas products from the rice straw pyrolysis experiment were analyzed using the following analytical methods. A PARR bomb calorimeter 6200 was used to measure high heating value (HHV) in accordance with ASTM D 711. The proximate and moisture data was obtained using ASTM standard D 3173 (Sample Preparation and Moisture Content Determination), D3175 (Standard Test Method for Volatile Matter for Ash in Biomass) and E1755 (Standard Test Method for Ash in Biomass) methods. Bio-oil from each reactor was analyzed according to ASTM standard D7544-10 which comprises of ASTM D482 (ash content) and E203 (water content). The pH of the bio-oil was measured using a digital pH meter. The ultimate analysis data (for C, H, N and S) was obtained from a Vario MICRO Elemental analyzer (ASTM D5373). A GC-MS of Shimadzu QP2010Plus, ZB5MS 30 m × 0.25 mm diameter × 0.25 μm thick, was used to determine chemical composition of the bio-oil. The column temperature was programmed at 40 °C and held for 5 min before this was ramped to 300 °C. The ramping was carried out at the rate of 5 °C/min and then held for 5 min. The gas composition was analyzed using an SRI Multiple gas chromatograph (GC) equipped with a TCD. The column in the GC contained a 6′ Molecular sieve 13X and a 6′ Silica Gel column. The carrier gas of helium was used to detect the gas mixtures of H_2, N_2, O_2, CO, CH_4, CO_2, C_2H_4, C_2H_6, C_3H_6, and C_3H_8. A Shimadzu IRAffinity-1 FTIR spectrophotometer was used to analyze the bio-oil. The mineral contents of samples were determined using ICP-OES of Spectro Blue, while the protein content was obtained from total nitrogen content which was determined by a high temperature combustion process.

2.4. Experimental design and data analysis

Three replications were used for each condition. The temperature was set at 500 °C in all the experiments, as the maximum bio-oil yield was obtained at this temperature [10,18,22,27,31]. The particle size of the rice straw was controlled by grinding the samples using a fixed sieve of 2 mm. The quantities of the feedstock used in each trial were about 250 g (batch reactor), 200 g (auger reactor) and 200 g fluidized bed reactor.

Pyrolysis using the auger type reactor is regarded as a slow or intermediate pyrolysis which is set at the speed of 1.03 RPM, and corresponds to the 20–25 min reaction time from Equation (1). The nitrogen gas flow was maintained at 10 L/min. For the slow pyrolysis, the reactor was heated at 4 °C/min until the set temperature (500 °C) and maintained for 30 min after nitrogen gas filled the reactor before each run. The residence time in the fluidized bed (FB) reactor was 1.6 s according to Equation (2) [8]. The inert gas flow rate of the fluidized bed reactor was set at 45 L/min.

$$\text{Residence time of the auger (s)} = \text{Auger reactor length (m)}/\text{Biomass flow velocity (m/s)} \quad (1)$$

$$\text{Residence time of the fluidized bed (s)} = \text{FB reactor volume (L)}/\text{Volumetric flow rate (L/s)} \quad (2)$$

Product mass and energy yields were obtained using Equations (3)–(5).

The yield balance was established after accounting for the losses. Mass yield was calculated on a weight basis whereas the energy yields of each of the solid, liquid, and gas product was calculated based on the amounts of energy converted from the initial biomass after pyrolysis.

$$\text{Product yield } (\%) = m_{product} / m_{initial} \quad (3)$$

$$\text{Bio} - \text{char yield } (\%) + \text{Liquid yield } (\%) + \text{Gas yield } (\%) + \text{Loss } (\%) = 100\% \quad (4)$$

$$\text{Energy yield } (\%) = \left(m_{product} \times HHV_{product}\right) / \left(m_{initial} \times HHV_{initial}\right) \quad (5)$$

3. Results and discussion

3.1. Rice straw characteristics

The properties of rice straw are shown in Table 1. The analysis showed the presence of a high proportion of volatile combustible matter (VCM) and ash, which contributed to about 69% and 22% of the rice straw used, respectively. The fixed carbon (FC) contents showed only 9%. These results are similar to those reported previously (60–79% VCM, 4.6–16% FC, and 9.8–23% ash) [12,13,18,32–34]. The presence of a large proportion of ash led to relatively low heating value (14.2 MJ/kg) compared to the reports of other studies (15–16.2 MJ/kg). This also affected the carbon and hydrogen concentrations, which were as low as 36% C and 4.9% H. The H/C and O/C molar ratios of RS were revealed as 1.61 and 0.65, respectively. This O/C molar ratio is less than that reported for corn stover (O/C 0.71) [10], but higher than those obtained from the algae *Nannochloropsis oculata* (O/C 0.39) [35]. The rice straw is expected to produce more oxygenated volatile compounds than *N. oculata*. The chemical composition of rice straw is: $CH_{1.61}O_{0.66}N_{0.02}S_{0.002}$.

3.2. Yields of pyrolysis products

Pyrolysis experiments were conducted to evaluate the effects of different reactors on product yield and characteristics with rice straw. Product mass yields of bio-char, liquid (bio-oil and aqueous phase) and the gas produced from an auger, a batch, and a fluidized bed reactor are shown in Fig. 2. The mass product yield from the auger and batch pyrolysis systems exhibit similar trends of highest yield of bio-char (45–48%), followed by the liquid product (25–31%) and then by the lowest yield of gas (11–13%). On the other hand, the highest yield of the liquid portion (43%) was obtained from the fluidized bed pyrolysis, followed by the bio-char (27%) and gas (23%). The mass yields of bio-char and liquid in fluidized bed and other reactors showed a complete reversal of the above results mainly due to the use of different heating rates. The fluidizing medium caused a broad and abrasive contact with biomass at a faster rate, resulted in a high yield of liquid portion. More of the direct heating surface of the fluidized bed medium would have converted the biomass into more volatile matters. Furthermore, the volatile matters did not have enough time, energy or both to decompose into gases at 500 °C [27]. On the other hand, high yields of bio-char were obtained from the slow pyrolysis process of auger and batch type reactors due to slower heat transfer rates to the biomass. Similar results were observed from the slow and fast pyrolysis studies. A mass product yield from rice straw pyrolysis processed at 500 °C and 1.2 s residence time produced 20% bio-char, and 36% liquid from a fluidized bed reactor [36]. A lab scale rice straw fast pyrolysis showed similar data at 23% bio-char, 50% bio-oil, and 27% gas at 520 °C [37]. In a slow pyrolysis process, about 40% bio-char, 38% bio-oil and 20% gas were obtained [12]. Thermogravimetric analysis (TGA) also showed 40% bio-char from rice straw pyrolysis [34]. The pyrolysis yields of corn stover in the same fixed bed reactors were reported at 32% for bio-char, 28% for liquid, and 18% for gas. Also, the bio-char output yield from the auger pyrolyzer gained around 50% by weight of biomass input [8].

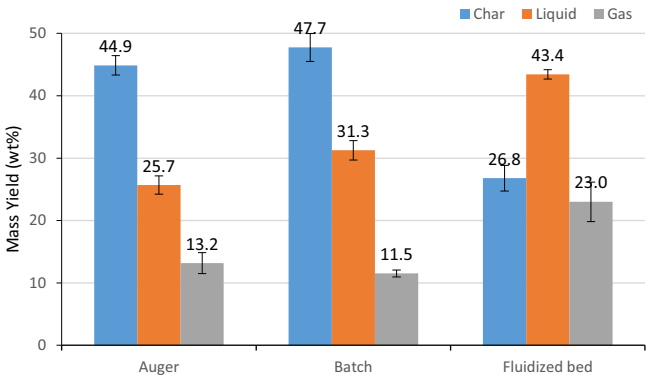

Fig. 2. Bio-char, liquid and gas product yields from rice straw pyrolysis.

Mass conversion efficiencies of different process reactors were calculated based on Equation (4). The average loss from each reactor was 35% for the auger, 9% for the batch, and 12% for the fluidized bed reactor. Those losses were generated mostly from uncondensed liquid bio-oils that remained on the sides of the reactors and pipes as well as uncollected bio-char and the gas. The auger reactor had the highest loss as the quantity of the samples used was too small in such a large scale equipment. Despite the weaknesses, the experimental data show a clear trend and they will be useful when developing a large-scale pyrolyzer for commercial applications. The auger type reactor for slow/intermediate rate pyrolysis has some technical advantages; it is easy to operate compared to fluidized bed reactor, and is also possesses faster production ability compared to a batch type reactor. Furthermore, the system can be automated, thus making it more user-friendly and cost effective.

Table 1
Rice straw and cotton stalk characteristics.

Biomass characteristics	Rice straw	Literature[a]
High Heating Value (MJ/kg), db	14.2 ± 0.2	15–16.2
Moisture (wt%)	9.2 ± 0.1	8.9–14.1
Proximate analysis (wt%), db		
VCM	69.3 ± 0.1	60–77
Fixed Carbon	9.01 ± 0.96	4.6–16
Ash	21.7 ± 1.1	9.8–23
Ultimate analysis (wt%), db		
C	36.6 ± 0.2	40.8–54
H	4.9 ± 0.15	5–7.6
N	0.77 ± 0.02	0.4–3.9
S	0.23 ± 0.02	0.5–0.56
O (by difference)	31.96	30–51.6

db: dry basis.
[a] [12,13,18,32–34].

3.3. Bio-oil properties

The liquid products from each reactor had different visual appearances. The bio-oil product from the FB reactor was homogenous and dark brown in color and produced a smoky odor. On the other hand, the liquid from the slow pyrolysis process of the auger and batch reactors separated into two layers of top organic portion (bio-oil) and a bottom aqueous portion (bio-liquor). The bio-oil composition contained alkanes, alkenes, alcohols, ketones, phenols, aromatics, and others in the top layer bio-oil from slow/intermediate pyrolysis and fast pyrolysis (Table 3). The top layer bio-oil from the slow pyrolysis process was more viscous and darker brown color than the bio-oil from fast pyrolysis process. The slow pyrolysis bio-oil smelled strong and irritating. The bottom layer

Table 2
Physicochemical properties of the pyrolysis bio-oil.

	Auger	Batch	FB	ASTM standard D7544	
HHV(MJ/kg)	29.4 ± 2.6	30.7 ± 2.1	20.6 ± 2.2	15 min.	ASTM D2015
Ash (wt.%)	<0.2	<0.2	1.0 ± 0.1	0.25max.	ASTM D482
pH	5.3 ± 0.3	3.1 ± 0.0	2.6 ± 0.1	Report	pH meter
MC content (wt.%)	14.3 ± 0.8	10.2 ± 0.3	5.7 ± 0.4	30max.	ASTM E203

Table 3
Chemical composition of bio-oil determined by GC–MS (**Bold** – name of chemical functional category).

Auger	Batch	FB
Compound (Relative %)	Compound (Relative %)	Compound (Relative %)
Alkanes (13.75)	**Alkanes (11.33)**	**Acids (4.27)**
Tridecane	Nonane	Acetic acid, methyl ester
Dodecane	Decane	Butanoic acid
Tridecane, 4,8-dimethyl-	Tridecane	Propanoic acid, 2-oxo-, methyl ester
Hexadecane	Dodecane, 2,6,11-trimethyl-	
		Alkenes (0.5)
Alkenes (8.88)	**Alkenes (10.18)**	3-Hexene
1-Dodecene	1-Decene, 4-methyl-	1-Butene, 3-methyl-3-(1-ethoxyethoxy)
3-Tetradecene, (Z)-	1-Dodecene	
1,4-Methanonaphthalene, 1,4-dihydro-	3-Tetradecene, (Z)-	**Alcohols (6.91)**
1-Tetradecene	2-Hexadecene, 2,6,10,14-tetramethyl-	2-Furanmethanol
1-Hexadecene	1-Tetradecene	1,4-Butanediol, 2,3-bis(methylene)-
1-Docosene		1,3-Propanediol, 2-(hydroxymethyl)-2-nitro-
	Alcohols (3.89)	1,3-Propanediol, 2-ethyl-2-(hydroxymethyl)-
Alcohols (4.83)	1,2-Ethanediol, diacetate	
Nonanol, 4,8-dimethyl-	2-Furanmethanol, tetrahydro-	**Ketones (17.72)**
2-Furanmethanol, tetrahydro-		1-Hydroxy-2-butanone
	Ketones (19.03)	2-Pentanone, 4-hydroxy-4-methyl-
Ketones (12.04)	2-Pentanone, 3-methyl-	4-Nonanone, 7-ethyl-
2-Cyclopenten-1-one, 2-methyl-	Cyclopentanone	Cyclohexanone
2-Cyclopenten-1-one, 3-methyl-	Cyclopentanone, 2-methyl-	2-Cyclopenten-1-one, 3-methyl-
2-Cyclopenten-1-one, 2,3-dimethyl-	Cyclopentanone, 3-methyl-	2-Furanone, 2,5-dihydro-3,5-dimethyl
Acetophenone	2-Cyclopenten-1-one, 2-methyl-	2-Cyclopenten-1-one, 3-ethyl-2-hydroxy
	2-Cyclopenten-1-one, 2,3-dimethyl-	
Phenols (35.27)	Cyclopentanone, 2-ethyl-	**Phenols (33.04)**
Phenol		Phenol
Phenol, 2-methyl-	**Phenols (27.72)**	Phenol, 2-methyl-
Phenol, 3-methyl-	Phenol	Phenol, 3-methyl-
Phenol, 2-methoxy-	Phenol, 2-methyl-	Phenol, 2-methoxy-
Phenol, 4-ethyl-	Phenol, 3-methyl-	Phenol, 4-ethyl-
Phenol, 2,3-dimethyl-	Phenol, 2-methoxy-	Phenol, 4-ethyl-2-methoxy-
Phenol, 2-ethyl-5-methyl-	Phenol, 2-methoxy-4-methyl-	Phenol, 2,6-dimethoxy-
	Phenol, 2,4-dimethyl-	Phenol, 2-methoxy
Aromatics (20.25)	Phenol, 4-ethyl-	Phenol, 2,6-dimethoxy-4-(2-propenyl)-
Ethylbenzene		Vanillin
Benzene, 1,2,3-trimethyl-	**Aromatics (25.27)**	1,2-Benzenediol
1H-Indene, 1-chloro-2,3-dihydro-	Ethylbenzene	1,2-Benzenediol, 4-methyl-
Benzene, 2-ethenyl-1,4-dimethyl-	p-Xylene	2-Methoxy-4-vinylphenol
Benzene, 1-ethyl-2-methyl-	Benzene, 1,3-dimethyl-	Hydroquinone
	Benzene, 1,2,4-trimethyl-	
Nitriles (4.43)	Benzene, 2-ethenyl-1,4-dimethyl-	**Aromatics (2.01)**
Benzonitrile	Benzene, 1-ethyl-2-methyl-	1,2,4-Trimethoxybenzene
	Toluene	1,3-Benzenediol, 2-methyl-
	Indene	
	1,4-Methanonaphthalene, 1,4-dihydro-	**Others (29.31)**
	Naphthalene	Furfural
		Benzofuran, 2,3-dihydro-
	Nitriles (1.56)	D-Allose
	Butanenitrile, 3-methyl-	Butanedial
	Pentanenitrile	Hexanedial
		3-Acetoxybenzaldehyde

aqueous portion was watery (less viscous) and yellowish in color. The separated liquid phase from slow pyrolysis was also reported from other biomass wastes of lignocellulose biomass [38–41] and aquatic wastes [35]. The bio-oil from fast pyrolysis also showed unseparated liquid in different studies [40,42]. However, invisible separation was found after a month of storage, and bottom portion had a higher portion (55%) of water than the middle or the top portions (23%) of bio-oil [42].

Fig. 3 shows the elemental compositions of pyrolytic bio-oils from three reactors. The highest carbon content (74%) of bio-oil was obtained from batch reactor, followed by auger reactor (61%), and fluidized bed reactor (50%). Conversely, the oxygen contents of bio-oil were 15% from the batch, 26% from the auger, and 42% from the FB reactor. The highest oxygen content was from the FB bio-oil which indicated the presence of oxygenated chemical compounds, as compared to the other two reactors. The trend in a higher oxygen content from the FB reactor to the fixed-bed (batch) type was also reported in a previous study [27]. Oxygen content of 21–28% was obtained from the fixed-bed reactor, whereas that of 30–48% was from the FB reactor. The presence of high oxygen content presents several weaknesses to the fuel; low heating value, unstable bio-oil, and immiscibility with other hydrocarbons [43]. The chemical formula for the three bio-oils are: $CH_{1.8}N_{0.04}O_{0.32}S_{0.005}$ (auger), $CH_{1.4}N_{0.03}O_{0.15}S_{0.004}$ (batch), and $CH_{1.6}N_{0.02}O_{0.62}S_{0.009}$ (FB). For a better understanding of the elemental composition of bio-oil, the Van Krevelen diagram was plotted as shown in Fig. 4. This diagram includes the results from the current study as well as many other studies [10,12,18,35,40,44,45]. The O/C ratios (0.03–0.62) of rice straw bio-oil from different reactors varied to a greater extent than did the H/C ratios (1.37–1.77). The previous pyrolysis studies from different feedstocks and reactors showed similar trends with the current study for H/C and O/C ratios. The bio-oil from the FB reactor had higher O/C ratio (0.58–0.74) compared to those from the batch reactor (O/C ratio of 0.07–0.29) and the auger reactor (O/C ratio of 0.32–0.59). The elemental ratio of the petroleum products are between 1.5 and 2.0 for H/C, and less than 0.06 for O/C [46]. The closest O/C ratio to a petroleum fuel was obtained from the batch reactor bio-oil (0.15). The results show that the pyrolysis oil needs further processing before it can substitute a petroleum oil. However, the mixing of bio-oil with petroleum products can be used without upgrading.

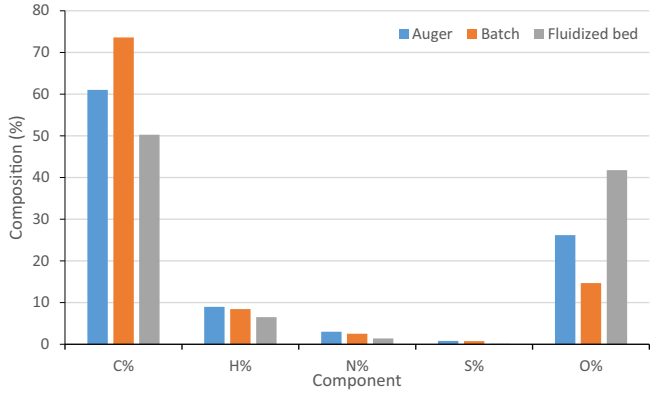

Fig. 3. Ultimate analysis of bio-oil from different reactors.

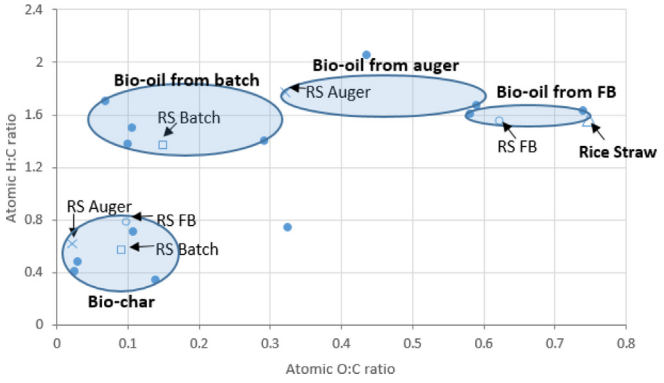

Fig. 4. Van Krevelen diagram for the liquid and solid products from different pyrolyzers (Reference of biomasses; corn stover, sorghum, rice straw, switchgrass, algae, and corn cob [10,12,18,35,40,44,45]).

Table 2 shows physicochemical characteristics of bio-oils. The high heating value (HHV) of bio-oil was found at 29 MJ/kg from the batch reactor, 31 MJ/kg from the auger reactor, and 21 MJ/kg from the FB reactor. These value were all above the ASTM standard of 15 MJ/kg. A high ash content of the fuels can contribute to wear of pumps, valves, and reactors by fouling and slagging. The ash content obtained from this study was less than 0.2 wt% from the slow/intermediate pyrolysis process, whereas 1.0 wt% in the FB bio-oil. The ash content of the bio-oil from an FB reactor can vary depending on the feedstock size and the reaction temperature [40]. The smaller the feedstock size and the lower the reaction temperature, the lesser will be the ash content was produced. A higher pH value from the auger pyrolysis bio-oil was determined at 5.3, which was higher than the bio-oils from the batch and the FB reactors. The bio-oil pH value which ranged between 2 and 4.5 was found from bagasse in a batch reactor, and from energy sorghum in an FB reactor [40,47]. As the low acidity is corrosive to metals, the low acidity should be treated before it is used in an engine. Moisture contents of bio-oils were determined at 14% from the auger, 10% from the batch, and 6% from the FB reactor. The amount of moisture present in the bio-oil affects the overall viscosity, the heat of combustion, and the flame temperature when used in the engines.

The relative chemical composition of bio-oil was determined using GCMS, and the results are shown in Table 3. More than 100 chemical compounds were detected in FB bio-oil, but a fewer number of chemical compounds were found in the bio-oils of auger and batch reactors. The compounds were categorized by chemical groups of phenols, alkanes, alkenes, alcohols, ketones, aromatics, nitriles, and others. The largest relative chemical from all three reactors was the phenol group at 28–35%. The 2-methoxyphenol is one of the main chemical compounds produced from the lignin portion of the biomass. More oxygenated compounds contributed to a higher phenolic content [48]. The phenol compounds were also found to be a major components of lignocellulose biomass [10,27,40]. Many oxygenated compounds of aromatics and ketones were produced mainly from cellulose and hemicellulose [49]. As the rice straw feedstock has high portion of glucan and xylan from the main components of cellulose and hemicellulose, respectively, a large percentage of the oxygenated chemicals were inevitably found in the derived bio-oils. Additionally, almost 20% of aliphatic compounds of alkanes and alkenes were obtained in the bio-oils of slow pyrolysis process whereas the bio-oil from the fast pyrolysis had only traces of aliphatic chemicals.

The FTIR spectra was used to understand the absorption of the functional groups of the bio-oil and aqueous product as shown in Fig. 5. The FTIR functional groups at each peak are referenced from other studies [10,35,50]. The peak ranged between 3600 and 3200 cm^{-1} which indicates that the O–H stretching vibrations show the presence of water, phenol, and alcohol, which was the dominant peak of the aqueous product from both the auger and batch pyrolysis processors due to the presence of large quantity of

water. The C–H bending vibration at 3200–2800 cm^{-1} and 1475–1350 cm^{-1} indicate the presence of alkanes in the bio-oils from both processes (2941, 1455, and 1380 cm^{-1}). The aliphatic acids that include ketones, aldehydes and carboxylic acids were detected in both the aqueous products and the bio-oils as the C=O vibration peaks from 1750 to 1650 cm^{-1}. A higher peak at 1654 cm^{-1} was observed in the aqueous product as compared to the bio-oil mainly by the wide spectrum bands of ketones, whereas a higher peak at 1710–1696 cm^{-1} was obtained in the bio-oil indicating the presence of aldehydes and carboxylic acid [51–53]. The C=C bending vibration peaks between 1650 and 1580 cm^{-1}, corresponding to the presence of alkenes and aromatic compounds were observed in both auger and batch type bio-oils (1600 cm^{-1}) as well as in the aqueous product (1640 cm^{-1}). The broad peak ranges of 1150–980 cm^{-1} (the C–O stretch of polysaccharides) [54], and 1215–1220 cm^{-1} (a strong vibration of C–C, C–O and C=O stretches) [55] were detected in the bio-oil, while no or small peaks in the ranges exist in the aqueous component. Polycyclic aromatics were found in the bio-oil (825 and 752 cm^{-1}) as the peaks between 900 and 675 cm^{-1}. This indicated the presence of polycyclic and substituted aromatic rings.

3.4. Bio-char properties

Bio-char samples were collected from the three process reactors. Proximate analysis of the bio-char from all reactors indicated the presence of the highest amount of ash content among others of the volatile combustible matter (VCM) and fixed carbon (FC) (Fig. 6; p-value 0.0185). It was reported that lignin was the main component of FC in the bio-char, which does not easily decompose at 500 °C [56]. As the pyrolysis temperature was set at 500 °C, a large portion of the VCM was reduced from 69% to 20–27% due to the removal of most of the cellulose and all of the hemicellulose. The FC from a batch reactor showed relatively higher amounts than other reactors (p-value 0.0023). This could be due to the pyrolysis reactions occurring statically in batch reactor, in comparison with that in a FB reactor where the reactions occur in the moving bed in N_2 flow. The conversion rate of lignin (FC) from the same materials can vary depending on the different process types. The heating value (HV) of the FB bio-char was 13 MJ/kg, whereas that from an auger and batch reactors was 16 (auger) and 19 (batch) MJ/kg. The higher heating value of the bio-char from the batch reactor as compared to the FB reactor can be explained by the sum of the VCM and FC contents.

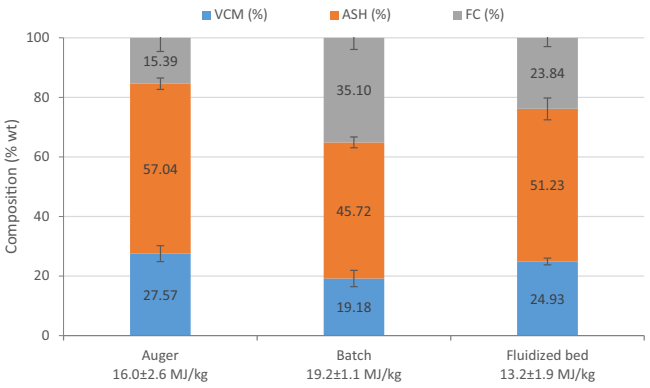

Fig. 6. Proximate data and high heating value for the bio-char products (dry basis).

The elemental compositions of bio-chars of different reactors were also determined. The carbon content was found to be between 38% and 45%, which was higher than that of rice straw (37%). As shown in the Van Krevelen plot in Fig. 4, the H/C (0.56–0.78) and O/C (0.02–0.1) ranges of rice straw bio-char did not vary much in spite of the use of different reactors. Also, the different feedstock (corn stover, sorghum, swith grass, algae, and corn cob) showed similar H/C (0.36–0.78) and O/C (0.03–0.32) ranges in the bio-chars. Thus, regardless of the type of feedstock and process reactors used, similar ratios of H/C and O/C were produced during the pyrolysis at around 500 °C as indicated in Fig. 7. However, the different operating temperatures from 200 to 300 °C lead to different ratios of H/C (0.89–1.65) and O/C (0.21–0.87) of rice straw and cotton stalk samples according to Nam and Capareda [13]. The highest bio-char carbon content was obtained from the batch pyrolysis, whereas the lowest was recorded from the auger bio-char. The protein contents of the bio-chars from the auger and batch reactors are (8.3%) as shown in Table 4, which verified the amount of nitrogen at 1.5% in bio-char from both reactors. The protein content of 2% from the FB reactor supported the nitrogen content of 0.49%.

Overall, the bio-char from the batch reactor has better quality for other power generation applications, as it has the lowest ash content, a high HV, and carbon content. Moisture content was found more or less about 1.5% ± 2 (auger), 1.7% ± 4 (batch), and 1.2% ± 5 (FB). The mineral content of P, K, Ca, Mg, Na, Zn, Fe, Cu, Mn, S, and B in the bio-char and raw rice straw was determined using

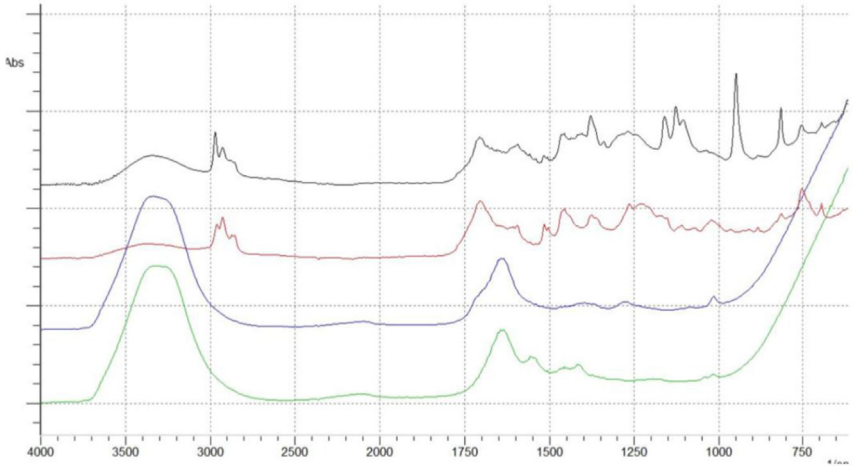

Fig. 5. FTIR of slow pyrolytic liquid fractions (from top; bio-oil from auger and batch, and aqueous portion from auger and batch).

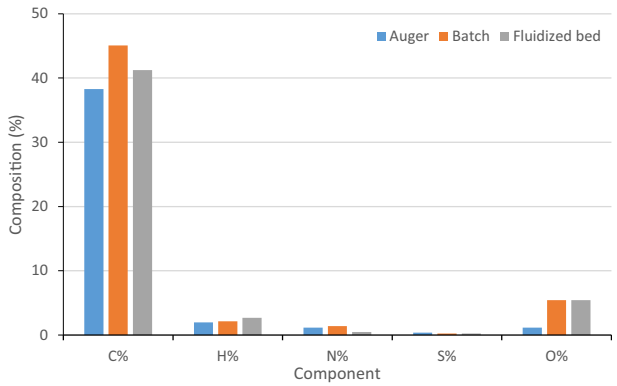

Fig. 7. Ultimate data of bio-char from the rice straw pyrolysis (dry basis).

ICP-OES as shown Table 4. The total mineral content differed by the type of reactor used: Raw RS (11.4 g/kg) < batch bio-char (41.2 g/kg) < FB bio-char (42.3 g/kg) < auger bio-char (46.9 g/kg). The highest alkali mineral contents of K, Ca, Mg, and Na were found in the auger bio-char (37.7 g/kg) as compared to batch bio-char (31.8 g/kg) and the FB bio-char (30.8 g/kg). The highest alkali content of auger bio-char can be utilized to correct soil acidity.

The X-ray diffraction patterns of bio-char were analyzed as shown in Fig. 8. The peaks in the bio-chars indicate the presence of inorganic materials of cristobalite (SiO_2), calcite ($CaCO_3$), and sylvite (KCl) [57,58]. The XRD patterns of auger and batch bio-chars are similar including the amorphous silica (cristobalite) broad peak at $\theta = 22.5°$. The peaks at $\theta = 28.3°$ and 40.4° were intensified, especially with auger RS bio-char, due to its high increase in potassium content compared to other bio-chars, which corresponds to the same results obtained from the ICP-OES analysis.

3.5. Gas composition

Combustible gas products were obtained from different reactors after pyrolysis as shown in Fig. 9. The composition of combustible gases were H_2, CO, CH_4, C_2H_2, C_2H_4, C_2H_6, C_3H_6, and C_3H_8. Since an N_2 carrier gas was used in the auger and fluidized bed, high N_2 gas composition was obtained in the product gas, which would have led to a low gas heating value of 7 (auger) and 0.4 (FB) MJ/m^3. As a study [59] reported that the minimum gas heating value of 4.2 MJ/Nm^3 is needed for engine use, the gas products from the batch and auger reactors may be applicable or

Table 4
Total mineral composition and protein contents of raw rice straw and pyrolysis bio-chars.

Dry basis	Raw RS	Auger RS bio-char	Batch RS bio-char	FB RS bio-char
Protein (wt.%)	0.9	8.3	8.3	2.0
P (mg/kg)	700	2900	2200	2600
K (mg/kg)	5000	24,500	19,400	17,400
Ca (mg/kg)	2200	8700	7600	7600
Mg (mg/kg)	1200	3900	4200	4600
Na (mg/kg)	390	634	550	1243
Zn (mg/kg)	27	198	130	93
Fe (mg/kg)	1209	1785	4106	7327
Cu (mg/kg)	19	99	17	143
Mn (mg/kg)	22	1656	1705	175
S (mg/kg)	625	2503	1241	1136
B (mg/kg)	3.6	18.5	9.8	11.3
Total Alkaline (g/kg)	8.8	37.7	31.8	30.8
Total Mineral (g/kg)	11.4	46.9	41.2	42.3

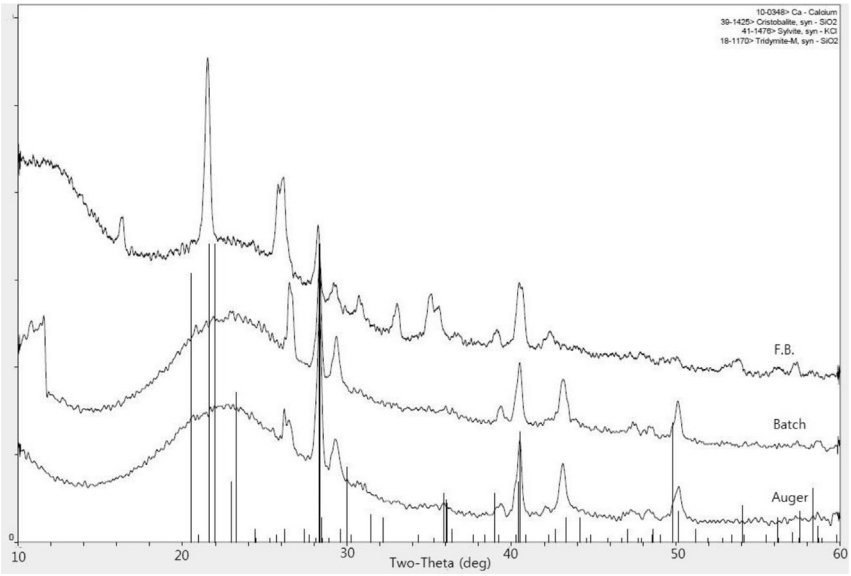

Fig. 8. XRD analysis of bio-char from auger, batch, and FB reactors.

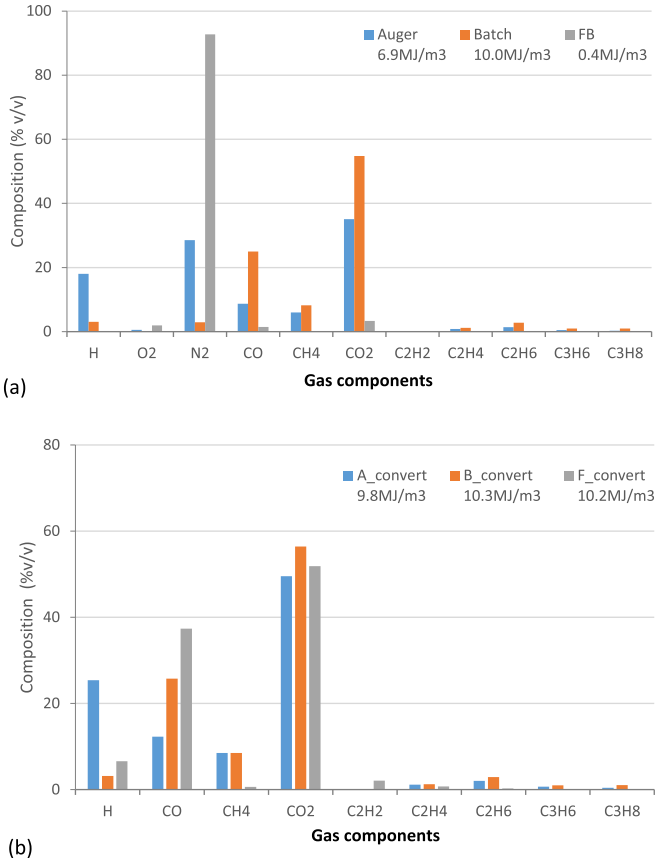

Fig. 9. Composition of gas product from the rice pyrolysis (a) as received (b) after removing O_2 and N_2 gases.

at least flammable. On the other hand, the gas from the FB reactor contained a large portion of non-combustible gas of about 95%. A high H_2 production from the auger pyrolyzer was noticeable among three reactors. Higher composition of H_2 gas can be obtained at the increased temperatures from the auger based reactor [60]. After calibrating the gas compositionsd by removing the O_2 and N_2 gases, the gas heating values from all reactors were increased to around 10 MJ/kg. Large amounts of CO and CO_2 gas production from pyrolysis process was produced by the cracking and reforming of functional carboxyl groups [35]. The gas heating values of batch reactor with a similar feedstock (corn stover) were reported to increase from 10 to 22 MJ/m^3 as the temperature increased from 400 to 600 °C [10].

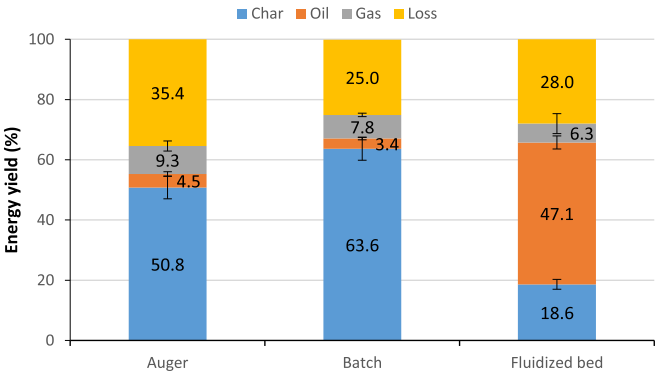

Fig. 10. Energy recoveries of pyrolysis process from different reactors.

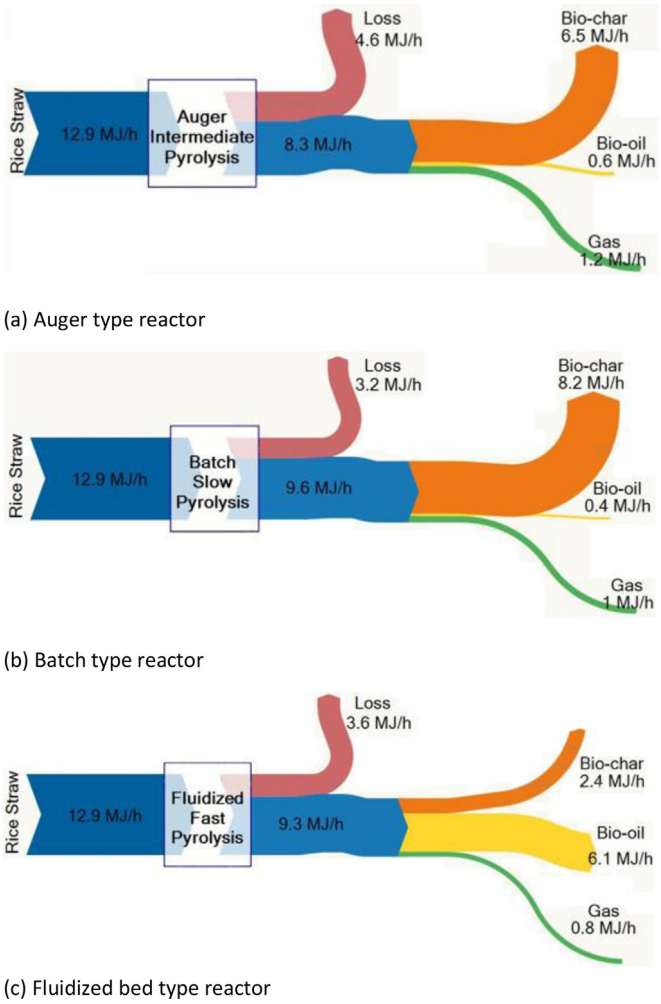

Fig. 11. Sankey diagram for bio-char, bio-oil, and bio-gas product distribution via various pyrolysis reactors.

3.6. Energy balance

Fig. 10 shows the energy recovery distribution of pyrolysis products from different reactors at 500 °C. It can be observed that the recovery of the energy yields were similar for batch and auger pyrolyzers. More than half of the initial energy was recovered by bio-char, and 10–15% of the energy was derived from volatile products (bio-oil and gas) in slow pyrolysis reactors. The low energy recovery of the volatile products is the result of the low quantities of bio-oil and non-combustible CO_2 gas. In contrast, the energy recovery from an FB bio-oil reached 47%, which was due to large mass production with moderate bio-oil heating value. On an average, the total energy recovered from these processes achieved ranged from 65% for the auger pyrolyzer to 75% for the batch pyrolyzer. Since the auger reactor was large, the energy loss was higher with the same amount of initial samples than with the other pyrolyzers. Otherwise, the product energy efficiency of the auger reactor was 81% [60]. Other researchers also reported energy loss as much as 25% and 18% during the pyrolysis process caused by reactor heat loss and energy lost from condensers [44,61]. The Sankey diagram helps in understanding how energy is transferred from raw biomass wastes to other types of products (bio-char, bio-oil, and bio-gas) as shown in Fig. 11. The process rate of biomass input was set at 1 kg/hour for three reactors, which

corresponds to 12.9 MJ/h. From the diagram, the energy of gas production from all types of reactors was close to 1 MJ/h. Large amounts of energy were contained in the solid products that were obtained from auger and batch reactors, while a major energy product from the FB reactor was bio-oil.

4. Conclusion

Three reactors (an auger type, a batch type, and a fluidized bed type) were utilized for the pyrolysis study. The temperature condition was set at 500 °C with 2 mm milled rice straw. The slow process of the auger and batch type reactors resulted in higher yields of bio-char, while the fast process of the fluidized bed reactor produced a larger quantity of bio-oil. The fast heat transfer rate due to the fluidizing medium led to a high mass yield of bio-oil. The heating value (HV) of bio-oils from the auger and batch type reactors showed a relatively higher HV than the fluidized bed reactor. The bio-oil from all reactors had a majority of phenolic compounds, and more aliphatic compounds were detected from the slow pyrolysis reactors. The bio-oil elemental composition ratio (O/C) showed different ranges depending on the type of reactor used, while the H/C ratio remained similar among the three reactors. On the other hand, both the O/C and H/C ratios of bio-chars were similar among three different reactors were obtained in similar ranges. In summary, a batch and an auger reactor can be recommended for bio-char production, whereas a fluidized bed reactor is optimal for bio-oil production even though the best bio-oil quality can be obtained from a batch reactor.

Acknowledgments

We gratefully thank Su-In Yi for his help on the XRD analysis.

References

[1] Bakker R, Elbersen HW, Poppens RP, Lesschen JP. Rice straw and wheat straw: potential feedstocks for the biobased economy. Utrecht, The Netherlands: NL Energy and Climate Change; 2013.
[2] FAOSTAT, Food and agriculture organization of the United Nations, 2012, 2014 (2012).
[3] Nelson RL, Thor PK, Heaton CR, Scheuring AF, Thompson OE, Garoyan L, et al. Rice straw burning: alternative policy implications. Order. 1980.
[4] Chang S, Zhao Z, Zheng A, He F, Huang Z, Li H. Characterization of products from torrefaction of sprucewood and bagasse in an auger reactor. Energy Fuels 2012;26:7009–17.
[5] Medic D, Darr M, Shah A, Potter B, Zimmerman J. Effects of torrefaction process parameters on biomass feedstock upgrading. Fuel 2012;91:147–54.
[6] Chen Y, Yang H, Yang Q, Hao H, Zhu B, Chen H. Torrefaction of agriculture straws and its application on biomass pyrolysis poly-generation. Bioresour Technol 2014;156:70–7.
[7] Lee J, Kim Y, Lee S, Lee H. Optimizing the torrefaction of mixed softwood by response surface methodology for biomass upgrading to high energy density. Bioresour Technol 2012;116:471–6.
[8] Capareda SC. Introduction to biomass energy conversions. Boca Raton, Florida: CRC Press, Taylor & Francis; 2014.
[9] Mahinpey N, Murugan P, Mani T, Raina R. Analysis of bio-oil, biogas, and biochar from pressurized pyrolysis of wheat straw using a tubular reactor. Energy Fuels 2009;23:2736–42.
[10] Capunitan JA, Capareda SC. Assessing the potential for biofuel production of corn stover pyrolysis using a pressurized batch reactor. Fuel 2012;95:563–72.
[11] Gui MSZ, Jourabchi SA, Ng HK, Gan S. Comparison of the yield and properties of bio-oil produced by slow and fast pyrolysis of rice husks and coconut shells. Appl Mech Mater 2014;625:626–9.
[12] Park J, Lee Y, Ryu C, Park Y. Slow pyrolysis of rice straw: analysis of products properties, carbon and energy yields. Bioresour Technol 2014;155:63–70.
[13] Nam H, Capareda S. Experimental investigation of torrefaction of two agricultural wastes of different composition using RSM (response surface methodology). Energy 2015;91:507–16.
[14] Puy N, Murillo R, Navarro MV, López JM, Rieradevall J, Fowler G, et al. Valorisation of forestry waste by pyrolysis in an auger reactor. Waste Manag 2011;31:1339–49.
[15] Sadaka S, Sharara M, Ubhi G. Performance assessment of an allothermal auger gasification system for on-farm grain drying. J Sustain Bioenergy Syst 2014;2014.
[16] Ashworth AJ, Sadaka SS, Allen FL, Sharara MA, Keyser PD. Influence of pyrolysis temperature and production conditions on switchgrass biochar for use as a soil amendment. BioResources 2014;9:7622–35.
[17] Ingram L, Mohan D, Bricka M, Steele P, Strobel D, Crocker D, et al. Pyrolysis of wood and bark in an auger reactor: physical properties and chemical analysis of the produced bio-oils. Energy Fuels 2007;22:614–25.
[18] Pütün AE, Apaydın E, Pütün E. Rice straw as a bio-oil source via pyrolysis and steam pyrolysis. Energy 2004;29:2171–80.
[19] Xiao R, Chen X, Wang F, Yu G. Pyrolysis pretreatment of biomass for entrained-flow gasification. Appl Energy 2010;87:149–55.
[20] Nam H, Maglinao A, Capareda S. Oxygen gasification and its syngas upgrading in a fluidized-bed reactor using sand mixed dairy manure. In: ASABE annual internation meeting conference proceeding; 2015. http://elibrary.asabe.org/abstract.asp?aid=45757&t=2&redir=&redirType=.
[21] Maglinao AL, Capareda SC, Nam H. Fluidized bed gasification of high tonnage sorghum, cotton gin trash and beef cattle manure: evaluation of synthesis gas production. Energy Convers Manag 2015;105:578–87.
[22] Pattiya A, Suttibak S. Influence of a glass wool hot vapour filter on yields and properties of bio-oil derived from rapid pyrolysis of paddy residues. Bioresour Technol 2012;116:107–13.
[23] Huang Y, Chen W, Chiueh P, Kuan W, Lo S. Microwave torrefaction of rice straw and pennisetum. Bioresour Technol 2012;123:1–7.
[24] Lam SS, Liew RK, Cheng CK, Chase HA. Catalytic microwave pyrolysis of waste engine oil using metallic pyrolysis char. Appl Catal B Environ 2015;176:601–17.
[25] Lam SS, Russell AD, Chase HA. Pyrolysis using microwave heating: a sustainable process for recycling used car engine oil. Ind Eng Chem Res 2010;49:10845–51.
[26] Lam SS, Chase HA. A review on waste to energy processes using microwave pyrolysis. Energies 2012;5:4209–32.
[27] Duman G, Okutucu C, Ucar S, Stahl R, Yanik J. The slow and fast pyrolysis of cherry seed. Bioresour Technol 2011;102:1869–78.
[28] Bainbridge D. Alternative uses of rice-straw in California. No.94–330. 1997.
[29] Grantz DA, Vaughn DL, Farber RJ, Kim B, Ashbaugh L, VanCuren T, et al. Transplanting native plants to revegetate abandoned farmland in the western Mojave Desert. J Environ Qual 1998;27:960–7.
[30] Bridgwater T. Biomass pyrolysis. EIA Report T34. 2007. p. 4. http://www.ieabioenergy.com/wp-content/uploads/2013/10/Task-34-Booklet.pdf.
[31] Lou R, Wu S, Lv G, Guo D. Pyrolytic products from rice straw and enzymatic/mild acidolysis lignin (EMAL). BioResources 2010;5:2184–94.
[32] Worasuwannarak N, Sonobe T, Tanthapanichakoon W. Pyrolysis behaviors of rice straw, rice husk, and corncob by TG-MS technique. J Anal Appl Pyrolysis 2007;78:265–71.
[33] Song C, Pawłowski A, Ji J, Shan S, Cao Y. Catalytic pyrolysis of rice straw and product analysis. Environ Prot Eng 2014;40.
[34] Chen G, Leung D. Experimental investigation of biomass waste,(rice straw, cotton stalk, and pine sawdust), pyrolysis characteristics. Energy Sources 2003;25:331–7.
[35] Maguyon MCC, Capareda SC. Evaluating the effects of temperature on pressurized pyrolysis of *nannochloropsis oculata* based on products yields and characteristics. Energy Convers Manag 2013;76:764–73.
[36] Eom I, Kim J, Lee S, Cho T, Yeo H, Choi J. Comparison of pyrolytic products produced from inorganic-rich and demineralized rice straw (Oryza sativa L.) by fluidized bed pyrolyzer for future biorefinery approach. Bioresour Technol 2013;128:664–72.
[37] Li R, Zhong Z, Jin B, Jiang X, Wang C, Zheng A. Influence of reaction conditions and red brick on fast pyrolysis of rice residue (husk and straw) in a spout-fluid bed. Can J Chem Eng 2012;90:1202–11.
[38] Carrier M, Hugo T, Gorgens J, Knoetze H. Comparison of slow and vacuum pyrolysis of sugar cane bagasse. J Anal Appl Pyrolysis 2011;90:18–26.
[39] Karaosmanoğlu F, Tetik E, Göllü E. Biofuel production using slow pyrolysis of the straw and stalk of the rapeseed plant. Fuel Process Technol 1999;59:1–12.
[40] Santos BS. Liquid-phase processing of fast pyrolysis bio-oil using platinum/HZSM-5 catalyst [ProQuest Dissertations and Theses]. 2013.
[41] Bae YJ, Ryu C, Jeon J, Park J, Suh DJ, Suh Y, et al. The characteristics of bio-oil produced from the pyrolysis of three marine macroalgae. Bioresour Technol 2011;102:3512–20.
[42] Manurung R, Wever DAZ, Wildschut J, Venderbosch RH, Hidayat H, van Dam JEG, et al. Valorisation of Jatropha curcas L. plant parts: nut shell conversion to fast pyrolysis oil. Food Bioprod Process 2009;87:187–96.
[43] Czernik S, Bridgwater A. Overview of applications of biomass fast pyrolysis oil. Energy Fuels 2004;18:590–8.
[44] Boateng AA, Daugaard DE, Goldberg NM, Hicks KB. Bench-scale fluidized-bed pyrolysis of switchgrass for bio-oil production. Ind Eng Chem Res 2007;46:1891–7.
[45] Zhang H, Xiao R, Huang H, Xiao G. Comparison of non-catalytic and catalytic fast pyrolysis of corncob in a fluidized bed reactor. Bioresour Technol 2009;100:1428–34.
[46] Wang C, Du Z, Pan J, Li J, Yang Z. Direct conversion of biomass to biopetroleum at low temperature. J Anal Appl Pyrolysis 2007;78:438–44.
[47] Asadullah M, Rahman MA, Ali MM, Rahman MS, Motin MA, Sultan MB, et al. Production of bio-oil from fixed bed pyrolysis of bagasse. Fuel 2007;86:2514–20.

[48] Li S, Chen X, Liu A, Wang L, Yu G. Study on co-pyrolysis characteristics of rice straw and Shenfu bituminous coal blends in a fixed bed reactor. Bioresour Technol 2014;155:252–7.
[49] Salehi E, Abedi J, Harding T. Bio-oil from sawdust: pyrolysis of sawdust in a fixed-bed system. Energy Fuels 2009;23:3767–72.
[50] Singh RK, Shadangi KP. Liquid fuel from castor seeds by pyrolysis. Fuel 2011;90:2538–44.
[51] Lievens C, Mourant D, He M, Gunawan R, Li X, Li C. An FT-IR spectroscopic study of carbonyl functionalities in bio-oils. Fuel 2011;90:3417–23.
[52] Bellamy LJ. Advances in infrared group frequencies The Infra-Red Spectra of Complex Molecules. 3rd ed. 1975. Chapman and Hall; New York: Wiley, London.
[53] Mayo DW, Miller FA, Hannah RW. Course Notes on the interpretation of infrared and Raman spectra. Hoboken, New Jersey: John Wiley & Sons; 2004.
[54] Stewart D, McDougall GJ, Baty A. Fourier-transform infrared micro-spectroscopy of anatomically different cells of flax (Linum usitatissimum) stems during development. J Agric Food Chem 1995;43:1853–8.
[55] Boeriu CG, Bravo D, Gosselink RJ, van Dam JE. Characterisation of structure-dependent functional properties of lignin with infrared spectroscopy. Ind Crops Prod 2004;20:205–18.
[56] Asadullah M, Zhang S, Li C. Evaluation of structural features of chars from pyrolysis of biomass of different particle sizes. Fuel Process Technol 2010;91:877–81.
[57] Wu W, Yang M, Feng Q, McGrouther K, Wang H, Lu H, et al. Chemical characterization of rice straw-derived biochar for soil amendment. Biomass Bioenergy 2012;47:268–76.
[58] Prakongkep N, Gilkes RJ, Wiriyakitnateekul W, Duangchan A, Darunsontaya T. The effects of pyrolysis conditions on the chemical and physical properties of Rice husk biochar. Int J Mate Sci 2013.
[59] Shah A, Srinivasan R, Filip To SD, Columbus EP. Performance and emissions of a spark-ignited engine driven generator on biomass based syngas. Bioresour Technol 2010;101:4656–61.
[60] Teiseh EA, Capareda S. Maximizing the concentrations of hydrogen, carbon monoxide and methane produced from the pyrolysis of a MixAlco process derived sludge. J Anal Appl Pyrolysis 2013;102:76–82.
[61] Mullen CA, Boateng AA, Goldberg NM, Lima IM, Laird DA, Hicks KB. Bio-oil and bio-char production from corn cobs and stover by fast pyrolysis. Biomass Bioenergy 2010;34:67–74.